applied sciences

MDPI

Article

Experimental Study on Interlayer Interference Characteristics During Commingled Production in a Multilayer Tight Sandstone Gas Reservoir

Yang Lu [1,*], Wenlin He [2], Jingjian Wang [3], Jiaojiao Liu [3], Hongguang Shi [2] and Daoyong Yang [4,*]

[1] School of Information Engineering, China University of Geosciences (Beijing), Beijing 100083, China
[2] National Key Laboratory of Petroleum Resources and Engineering, China University of Petroleum (Beijing), Beijing 102249, China; queenhe_1022@sina.com (W.H.); petershi_1022@sina.com (H.S.)
[3] Research Institute of Petroleum Exploration and Development, Changqing Oilfield Company, CNPC, Xi'an 710018, China; tomywang_7100@yeah.net (J.W.); mialiu_7100@yeah.net (J.L.)
[4] Energy Systems Engineering, Faculty of Engineering and Applied Science, University of Regina, Regina, SK S4S 0A2, Canada
* Correspondence: luyang@cugb.edu.cn (Y.L.); tony.yang@uregina.ca (D.Y.)

Abstract: In this study, a practical and comprehensive experimental technique has been proposed to investigate the interlayer interference characteristics in multilayer tight sandstone gas reservoirs with multi-pressure systems and different reserves. Firstly, single-layer depletion simulation experiments were conducted to measure the gas flow rate and gas extraction efficiency for each of the six layers. A series of physical simulation experiments were then conducted to monitor gas production and pressure variations in commingled multilayer production scenarios under various conditions. Finally, interlayer interference characteristics and gas extraction efficiencies and the main controlling factors were evaluated, analyzed, and identified. The interlayer pressure differential is found to be the primary factor dictating both interference and gas production, followed by initial gas production rates, and permeability variations in the order of positive significance. A higher interlayer pressure differential, a lower initial gas production rate, and a larger permeability variation result in an increase in interlayer interference and a reduction in gas production during commingled production. Increasing the number of commingled layers leads to an overall increase in gas production losses of 10.95% for two layers to 13.35% for four layers. Layers exhibiting small interlayer pressure difference are positively compatible for commingled production.

Keywords: tight sandstone gas reservoir; commingled multilayer production; physical simulation experiment; interlayer interference; controlling factors

Citation: Lu, Y.; He, W.; Wang, J.; Liu, J.; Shi, H.; Yang, D. Experimental Study on Interlayer Interference Characteristics During Commingled Production in a Multilayer Tight Sandstone Gas Reservoir. *Appl. Sci.* **2024**, *14*, 10534. https://doi.org/10.3390/app142210534

Academic Editor: Nikolaos Koukouzas

Received: 29 October 2024
Revised: 13 November 2024
Accepted: 13 November 2024
Published: 15 November 2024

1. Introduction

The ED Basin is a significant production area of tight gas in China with a total gas reserve up to 10.37 × 10^{12} Sm^3, indicating a promising and sustainable potential for exploration and development [1–3]. Although the gas reservoirs in the eastern region of the ED Basin are vertically superimposed in multiple layers with their stable distributions, each of the individual layers is relatively thin with a small reserve [4]. The single-layer development of these multilayer tight gas reservoirs often falls short of achieving industrial or commercial production capacity and yields subpar economic benefits, thus necessitating the implementation of commingled multilayer production [5,6]. Both the heterogeneity of these reservoirs and their significant pressure differentials between layers, however, result in interlayer gas backflow and uneven reserve utilization in commingled multilayer production, ultimately leading to a reduction in gas output compared to the cumulative production from single-layer development [7,8]. Therefore, it is of a practical significance to delineate interlayer interference characteristics and determine the reasonable multilayer development strategies in the ED Basin.

In practice, commingled multilayer production involves employing reasonable completion techniques within a single wellbore to effectively and efficiently extract gas from multiple vertically superimposed reservoirs, thereby optimizing gas yield and offsetting drilling expenses [9]. Due to differences in sedimentary depositions, diagenesis, and other factors between gas layers, not only do the porosity, permeability, and pore-throat structure of each layer vary significantly, but also the effect of pressure differences between any two vertical layers is noticeable [10,11]. During commingled multilayer production, significant variations in reservoir pressure and pressure coefficients between different layers result in fluids flowing back from a high-pressure layer into a low-pressure one, causing interlayer crossflow and thus affecting the production contribution and recovery factor of each layer [12,13]. The commingled exploitation scheme, together with the prorated flow rate of each layer, imposes an impact on the degree of interlayer interference, productivity together with its dynamic variation characteristics, and recovery efficiency [14,15].

Physical simulation experiments allow us to visualize the interlayer interference between various layers during commingled multilayer production. In practice, gas depletion experiments were conducted by employing two or three single-core plugs in a parallel manner to simulate the commingled production of multiple gas layers, aiming to instantaneously investigate the impact of pressure, permeability, and other factors on the interlayer interference, gas flow rate, and recovery efficiency for each layer [16]. To ensure the consistent petrophysical properties of the inherent randomness of a single-core plug, an elongated core plug was cut into multiple short ones to simulate a specific production layer, thereby enhancing the accuracy of simulating gas flow between various layers during commingled multilayer production [17]. Based on permeability and pressure difference, together with the contribution ratio of gas production during commingled coalbed methane production, a framework for assessing the associated compatibility was proposed [18]. To quantify the degree of interlayer interference during commingled multilayer production, the concept of an interlayer interference coefficient was proposed based on actual gas well production data [19–21]. So far, not only have no systematic attempts been made to physically simulate commingled multilayer production by taking the petrophysical properties, pore-throat structure, pressure, and controlled reserves of each layer into account, but also no methods have been proposed to evaluate the extent of interlayer interference in physical simulation experiments.

In this paper, a pragmatic and systematic method has been presented to experimentally characterize the interference of multiple gas layers with low permeability in the eastern ED Basin. The core combination schemes and experimental parameters for each layer were initially determined based on the measured petrophysical properties, pore-throat structure, pressure, and reserves. The single-layer depletion experiments were subsequently conducted for each layer with the aim of analyzing the dynamics of gas rate and pressure as well as recovery efficiency under single-layer conditions, which would serve as a comparative basis for evaluating commingled multilayer production potential. During the physical simulation experiments, the gas rate and pressure variations of each layer were measured for two-, three-, and four-layer commingled production, respectively. By comparing the recovery efficiency from single-layer and commingled multilayer production, a quantitative evaluation method was proposed and employed to assess the degree and patterns of interlayer interference, thereby evaluating the compatibility of each layer for commingled production.

2. Experimental

2.1. Materials

A total of 203 conventional core plug samples with a diameter of 2.54 cm and a length of 4.00 cm to 7.00 cm were collected from six members of Q5, H8, S1, S2, TY, and BX, which are the main gas-bearing members in this sandstone reservoir, located in the Mesozoic Permian and Upper Paleozoic Carboniferous strata, and which represent the main gas-producing layers in the east ED Basin, China [22]. In order to enhance the

comparability of the commingled multilayer production via actual gas wells, experiments were conducted using a long cylindrical core plug with a diameter of 2.54 cm to simulate the production performance of each gas layer. A long core plug was created by splicing multiple conventional core plugs along the axis, while its length was determined based on a comprehensive calculation considering parameters such as pressure, porosity, and reserve ratio between layers. The porosity and permeability of all these conventional samples were measured, of which 57 samples with similar petrophysical properties in the corresponding layers were prepared for splicing long core plugs for commingled multilayer production experiments. The purity of the research-grade helium and nitrogen used for measuring porosity and permeability was 99.999 mol%. In addition to using this nitrogen as the experimental fluid, a synthetic brine with a salinity of 55,000 mg/L, consisting of 7.00 wt% NaCl, 0.60 wt% $CaCl_2$, and 0.40 wt% $MgCl_2$, was prepared and utilized as reservoir brine to mitigate the influence of water sensitivity.

2.2. Experimental Setup

The schematic diagram in Figure 1 illustrates the experimental setup for the physical simulation of three-layer combined production in tight gas reservoirs. It is worth noting that the number of simulated layers corresponds to the number of long coreholders utilized in these experiments. This study involved simulations ranging from one to four layers of combined production, indicating simultaneous utilization of one to four long coreholders.

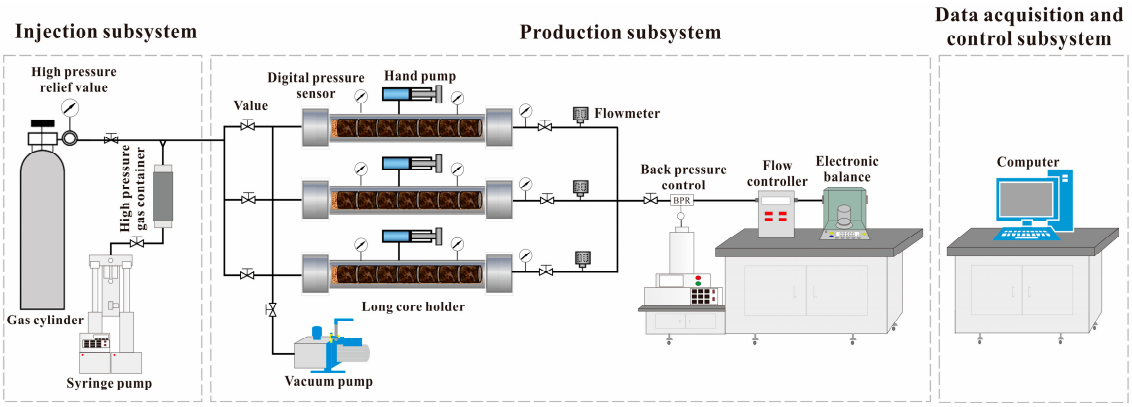

Figure 1. Schematic diagram of the experimental setup used for commingled multilayer production.

The experimental setup consisted of three subsystems, i.e., the injection subsystem, production subsystem, and data acquisition and control subsystem. In the injection subsystem, a high-pressure gas cylinder (WMA219-40-15, 40 L) was utilized to supply gas to the transfer cylinder. A high-pressure syringe pump (100 DX, ISCO Inc., Lincoln, NE, USA) was employed for injecting gas from the transfer cylinder into the core plugs contained in the coreholders (DCD-80b, Hai'an County Petroleum Scientific Research Instruments Co., Ltd., Nantong, China) in the production subsystem at various pressures. These long coreholders, within which the cylindrical cores at each layer were horizontally assembled, were capable of accommodating a core plug with a length of up to 80 cm. To provide confining pressure for the core plugs, a high-pressure manual pump (JB-II, Hai'an, China) was used with an additional 2.00 MPa above the injection pressure setting. Initially, a vacuum pump (FY-4c-N, Nantong, China) was employed to evacuate the cores and remove the impurities. Each long coreholder was equipped with three digital pressure gauges (3051TG, Rosemount, Chanhassen, MN, USA) at its inlet, middle, and outlet, each of which had a pressure range of 0–69 MPa and an accuracy of 0.025% full-scale. Also, a flow controller was employed to regulate the total gas flow rate during the depletion of one or multiple long core plugs. A back pressure regulator (BPR) (HY-2, Nantong, China) primarily controlled the ultimate outlet pressure, while several mass flowmeters (DMF-1-1, Beijing Shouke Shihua Automation Equipment Co., Ltd., Beijing, China) with a pressure range of 0–40 MPa

and an accuracy of ±(0.8% reading + 0.2% full-scale) were utilized for real-time monitoring and measuring the flow rates of each individual layer. The data acquisition and control subsystem enabled most data collection and experimental operations to be continuously monitored and measured via a desktop computer, thereby minimizing experimental errors associated with manual operations.

2.3. Experimental Procedures

2.3.1. Initial and Production Conditions

The experimental parameters for the primary gas-producing layers Q5, H8, S1, S2, TY, and BX were determined based on the porosity, permeability, pressure, and reserves. The permeability and porosity of each layer were measured after the conventional core plugs were spliced into a continuous long core plug. Table 1 presents the petrophysical properties, pore pressure, length of the spliced long core plug, and initial gas flow rate for each layer.

Table 1. Experimental parameters for single-layer gas depletion and commingled multilayer production of each layer.

Layer	Permeability (mD)	Porosity (%)	Pressure (MPa)	Diameter of Long Core (cm)	Length of Long Core (cm)	Initial Gas Production Rate (mL/min)	Abandonment Pressure (MPa)
Q5	0.76	8.17	7.30	2.54	47.40	2.30	0.50
H8	0.66	7.80	22.00	2.54	43.00	3.00	
S1	0.45	6.05	22.60	2.54	42.40	3.70	
S2	0.54	6.90	22.80	2.54	49.00	2.40	
TY	0.56	8.70	23.41	2.54	43.40	2.80	
BX	0.85	7.08	25.00	2.54	22.00	3.10	

The single-layer gas depletion experiments can be directly conducted using the corresponding parameters provided in Table 1; however, when conducting commingled production experiments, it is crucial to aggregate the gas production rate of each layer. For example, in the case of commingled production for Q5 and H8 layers, the gas production rate needs to be summed up to 5.30 mL/min.

2.3.2. Depletion Experiments of Single-Layer and Multilayer Cores

The single-layer depletion experiments were initially conducted for the six layers with the experiment parameters tabulated in Table 1. The variations in flow rate, pressure, cumulative gas volume, and total gas production were then obtained. Subsequently, commingled simulation experiments were conducted for two layers, three layers, and four layers, respectively. The commingled two-layer experiments were conducted in three groups, utilizing the Q5 + H8, H8 + BX, and S1 + TY combinations. The commingled three-layer experiments were carried out in four groups, i.e., Q5 + S2 + TY, Q5 + H8 + S2, H8 + S2 + TY, and S2 + TY + BX combinations. The commingled four-layer production experiments were then executed in three groups, i.e., Q5 + H8 + S1 + TY, H8 + S1 + S2 + TY, and H8 + S2 + TY + BX combinations. It is worthwhile mentioning that the aforementioned experiments were conducted at an atmospheric temperature of 25 °C.

The procedure of conducting commingled multilayer experiments is exemplified by the using the three-layer (i.e., Q5 + H8 + S1) scheme, i.e.,

(1) The three spliced long core plugs were placed in the three long coreholders to simulate three layers with varying petrophysical characteristics.
(2) Each of the three vacuumed long core plugs were saturated separately by injecting nitrogen in a constant injection pressure mode according to the pressure of each individual layer in the targeted tight gas reservoir. The initial flow pressures of Q5, H8, and S1 were, respectively, set to be 7.30 MPa, 22.00 MPa, and 22.60 MPa to simulate gas production performance in the targeted multi-pressure tight gas reservoir.

During each experiment, the confining pressure was set to be 2.00 MPa higher than the initial pressure.

(3) Upper experimental flow rate limit at the outlet was controlled to be the summation of each layer of 9.00 mL/min for the selected three layers by using the gas flow controller to perform constant rate depletion, simulating the commingled production in the multi-pressure system of tight sandstone gas reservoirs. When the gas flow rate could not be maintained at 9.00 mL/min, the experiment was terminated using the outlet valves, based on the abandonment pressure of 0.50 MPa.

(4) The pressure, production time, and in situ gas production of each layer were monitored and recorded continuously until the end of the experiments, during which pressure at the inlet, middle, and outlet were monitored and recorded continuously.

3. Results and Discussion

3.1. Commingled Production Characteristics

During commingled multilayer production experiments, the total gas flow rate remained stable at its preset value under the constant flow rate at the outlet, and then gradually decreased until reaching its abandonment pressure. From the total gas production curve of the commingled Q5 + H8 layers shown in Figure 2a, it can be seen that the total gas production remained at the preset flow rate of 5.3 mL/min throughout the entire experiment duration until 1234 min. Afterward, the gas production rate of the commingled two-layer production began to gradually decline, ultimately reaching the abandonment pressure of 0.50 MPa at 1718 min, marking the termination of the experiment.

Although the total gas production remained constant during the period from the very beginning to 1234 min, the productions from each individual layer Q5 or H8 underwent a complex stage with an initial interlayer interference followed by joint gas production. Due to the pressure difference between interlayers, gas was not discharged from the low-pressure layer during the initial stages of production. Moreover, gas from the high-pressure layer not only flowed out of its outlet, but also flowed back into the low-pressure layer. By analyzing the curves of instantaneous gas production and gas contribution rate over time for the commingled Q5 + H8 layer production, it is evident that, within the initial 169 min of extraction, not only did the high-pressure layer H8 exclusively contribute to gas production at its outlet, but there was also a reverse flow of gases from layer H8 into the low-pressure layer Q5, resulting in a negative actual gas contribution from the latter. After 169 min, the instantaneous gas production rate and gas contribution ratio of the layer H8 exhibited a gradual decline, while the gas production rate of the layer Q5 was transitioned from negative to positive, initiating gas generation and its subsequent stabilization (see Figure 2a,b).

The comparison of the commingled H8 + BX layer production curves depicted in Figure 3a,b reveals that significant disparities in interlayer pressure would lead to an extended phase of stable production with interference; however, when the interlayer pressure is closely matched between the two layers, the duration of the interference-stable production phase is reduced.

Based on the gas production characteristics of the aforementioned commingled two-layer production, the gas production characteristics of commingled multilayer production at the constant outlet flow rate can be categorized into three production stages, i.e., production with stable interference between layers, stable production from commingled layers, and declining production from commingled layers, while their corresponding time frames for commingled Q5 + H8 layer production are found to be from 0–169 min, 170–1234 min, and 1235–1718 min, respectively (see Figure 2a). The time frames corresponding to the three stages for the H8 + BX layers shown in Figure 3a,b exhibit smaller interlayer pressure differences, i.e., 0–11 min, 12–1479 min, and 1480–1795 min, respectively. When more layers are involved in commingled production, the significant characteristics of the three stages persist. Figure 4a,b illustrates the characteristic curve of commingled four-layer H8 + S2 + TY + BX production, wherein the aforementioned three production

stages remain distinctly observable with their corresponding time frames of 0–16 min, 17–1873 min, and 1874–2162 min.

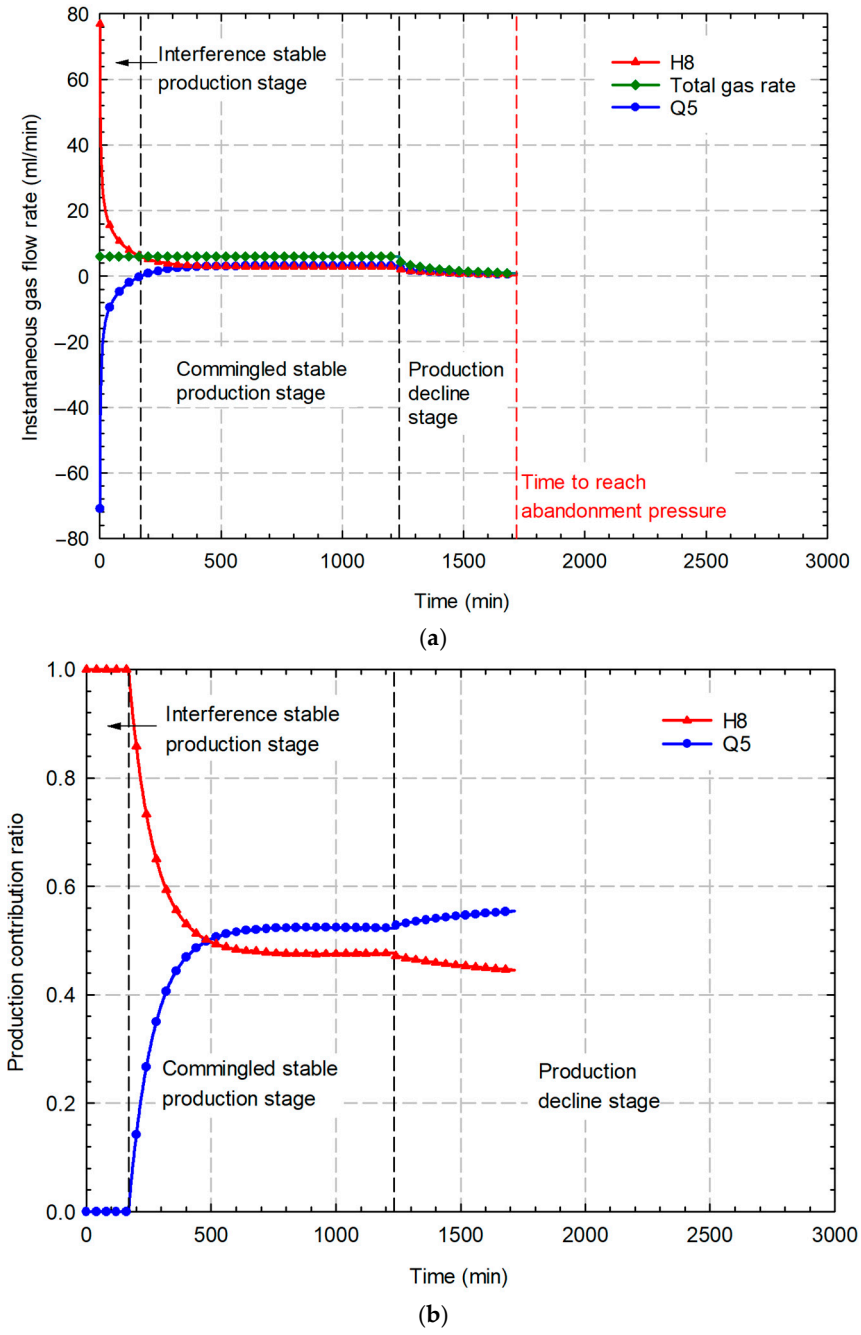

Figure 2. (**a**) Instantaneous gas flow rate and (**b**) production contribution ratio curves for the commingled production of Q5 + H8 layers.

3.2. Interlayer Interference Time and Backflow Gas Volume

The interlayer interference time is defined as the total duration from the beginning of commingled multilayer production to the complete discharge of backflowed gas from the low-pressure layer, and it encompasses the duration of the backflow from a high-pressure layer to a low-pressure one and backflowed gas discharge from the low-pressure one. In other words, the termination of interlayer interference coincides with the initiation of discharge for the original gas saturation in the low-pressure layer. The backflow duration refers to the period during which gas in a high-pressure layer enters a low-pressure layer, corresponding to the duration of the previously mentioned production stage with stable

interference between interlayers. The backflow gas discharge time refers to the duration starting from the time at which backflowed gas from the high-pressure layer is being produced from the low-pressure layer until all the backflowed gas is completely discharged.

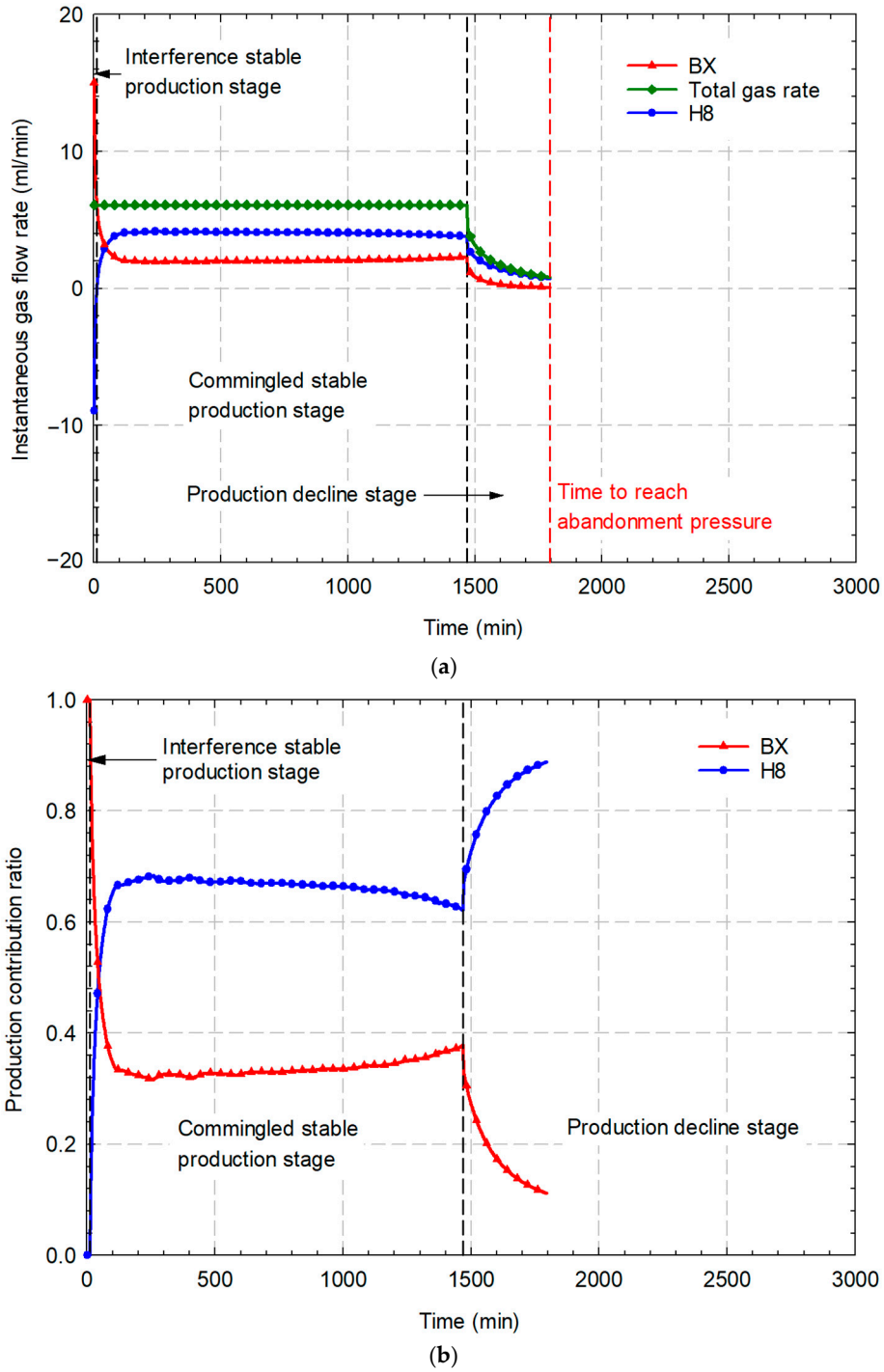

Figure 3. (**a**) Instantaneous gas flow rate and (**b**) production contribution ratio curves for the commingled production of H8 + BX layers.

Due to the significant differences in interlayer pressure and properties, the backflow time and gas discharge time were prolonged during the commingled Q5 + H8 layer production. The pressure and cumulative gas production variation curve during the commingled Q5 + H8 layer production, as depicted in Figure 5a,b, illustrates that the Q5 layer experienced backflow with an increase in pressure and that there was a rapid

decrease in pressure on the H8 layer. The backflow duration was 169 min, accounting for 9.84% of the total production time of 1718 min. The backflow gas volume from layer H8 to layer Q5 amounted to a total of 1511 mL under standard conditions, representing 61.17% of the initial gas content in layer Q5. The maximum instantaneous backflow rate can reach 70.93 mL/min, which is equivalent to 13.38 times the total gas rate at the outlet. The pressure between the two layers gradually approached equilibrium, entering a stable production stage where both Q5 and H8 layers commenced simultaneous gas production, resulting in a concurrent reduction in pressure. At 752 min, the gas backflowing into layer Q5 was completely produced. The total duration of backflow and backflowed gas discharge time amounted to 752 min, representing 43.79% of the total gas discharge time of 1718 min.

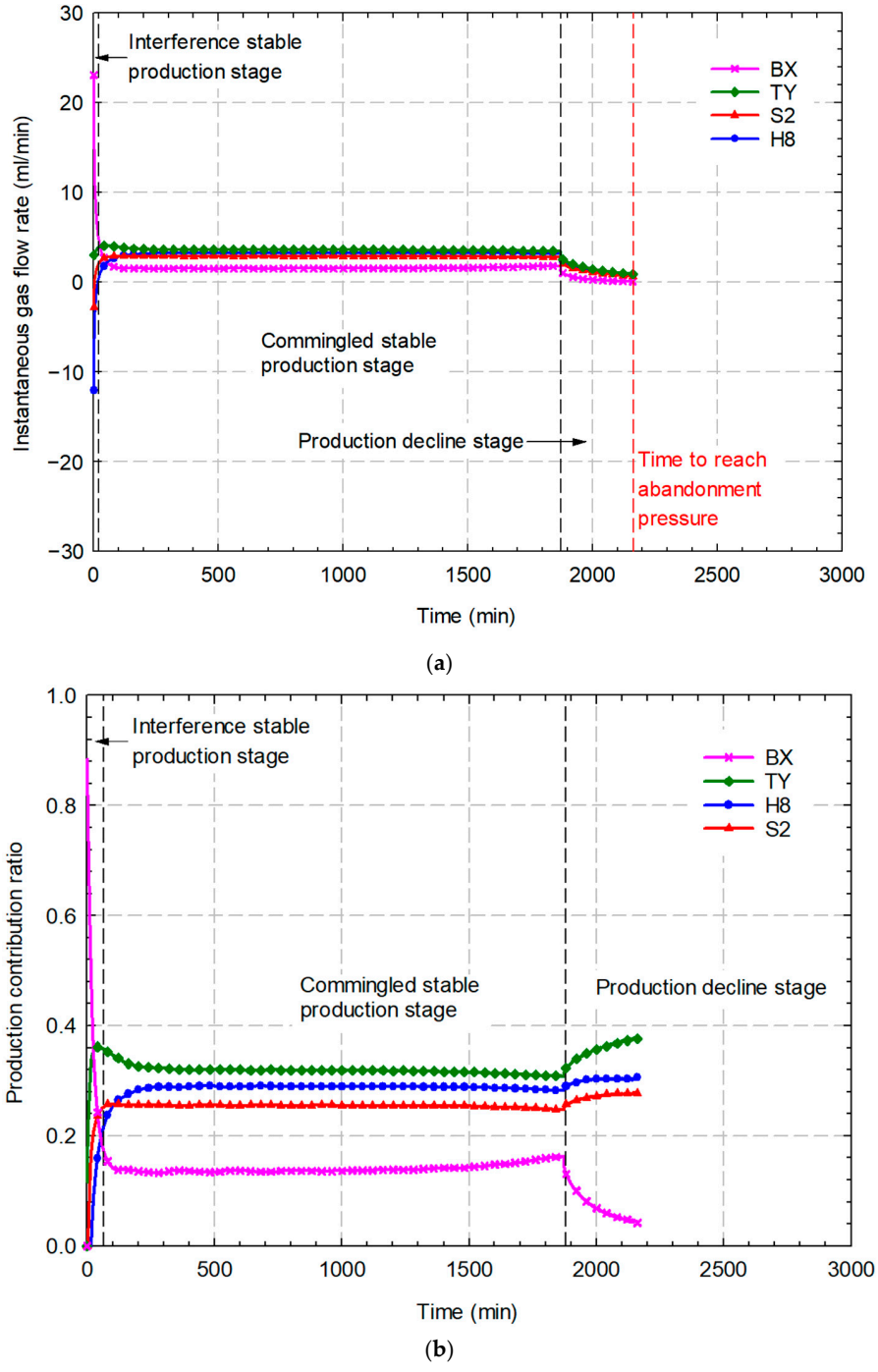

Figure 4. (**a**) Instantaneous gas flow rate and (**b**) production contribution ratio curves for the commingled production of four layers.

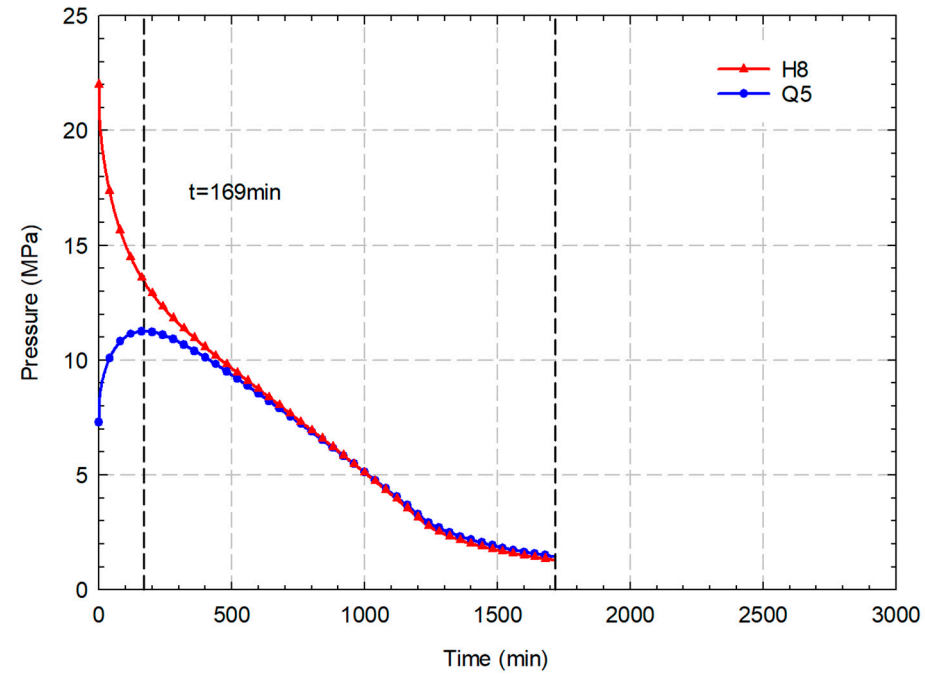

(**a**)

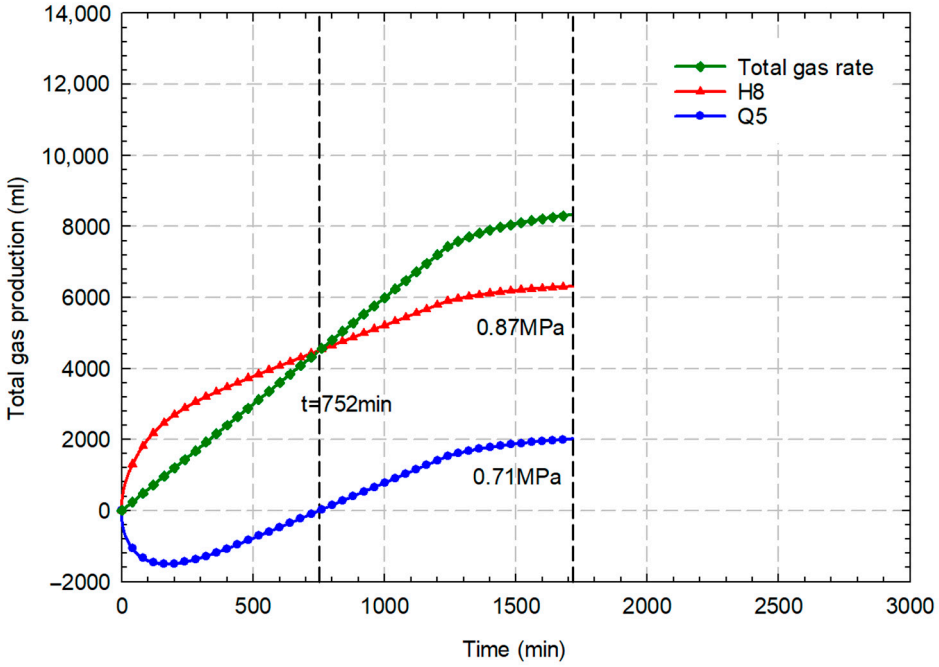

(**b**)

Figure 5. (**a**) Pressure change and (**b**) accumulated gas production curves for the commingled production of Q5 + H8 layers.

The interlayer difference in H8 + BX layers was relatively smaller compared to that of Q5 + H8 layers. Although there was interlayer interference during commingled two-layer production, the duration of interference was relatively short in comparison to that of the total gas discharge time. As can be seen in Figure 6a,b for the commingled H8 + BX layer production, the durations of backflow and subsequent backflowed gas discharge were found to be 11 min and 41 min, respectively, accounting for a mere 0.61% and 2.28% of the total gas discharge time. The backflow gas volume and rate were relatively low, with a maximum backflow rate of merely 1.46 times the total gas production rate, while the

corresponding backflow volume accounted for only 0.88% of the initial gas content. Such a backflow phenomenon was not prominent in the commingled S1 + TY layer production due to unobvious interlayer pressure differences, and both the backflow rate and volume were minimal.

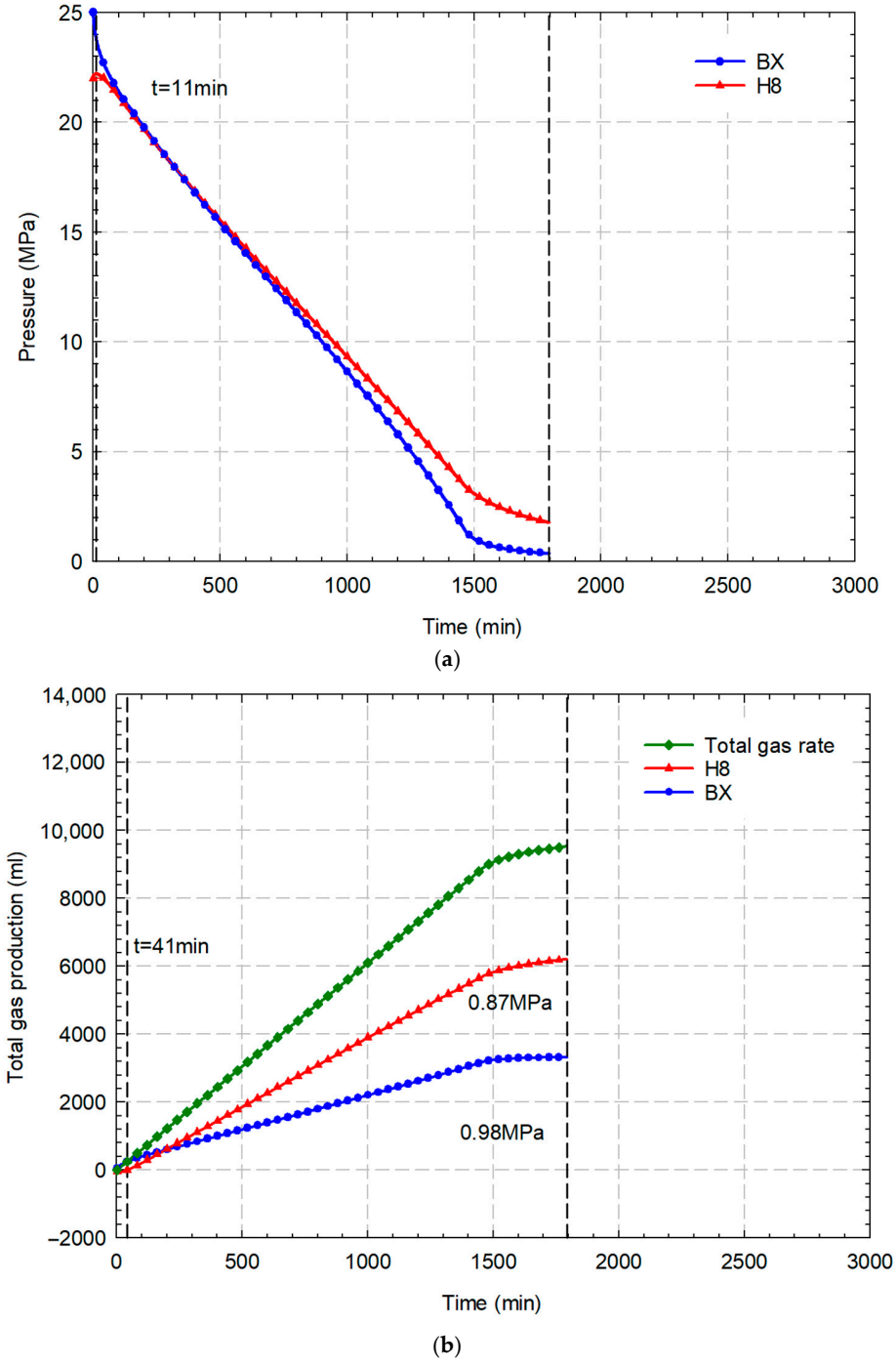

Figure 6. (**a**) Pressure change and (**b**) accumulated gas production curves for the commingled production of H8 + BX layers.

The above analysis reveals that, in the presence of a significant difference in interlayer pressure, there exists an increase in both gas backflow volume and maximum instantaneous backflow rate. Also, there is an extension observed in the duration of backflow and interlayer interference time. The results presented in Figure 7a demonstrate that a larger pressure difference between layers during commingled two-layer production leads to an

increase in backflow time, ratio of backflow time to total gas discharge time, and ratio of backflow gas discharge time to total gas discharge time, respectively. Such an observed pattern remains distinguishably in the commingled three-layer production depicted in Figure 7b. The time statistics for experiments with commingled production for two, three, and four layers are listed in Table 2, from which it is evident that, as the pressure differential increases under the commingled production from the same layer, there is a significant prolongation of interlayer interference time that also constitutes a higher proportion of total gas production time.

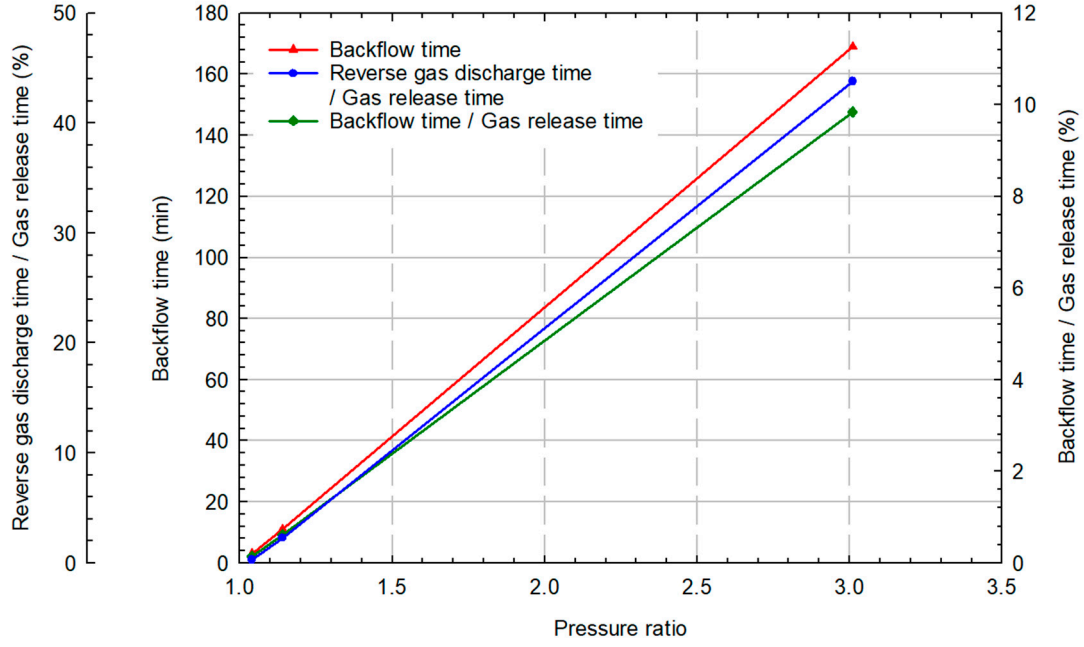

(**a**)

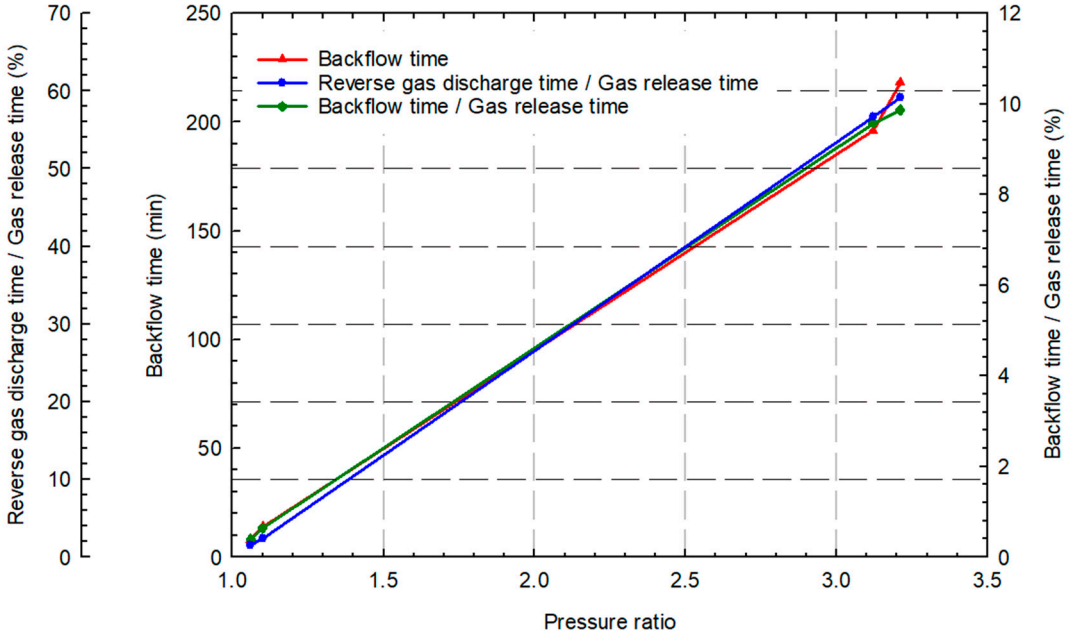

(**b**)

Figure 7. Backflow time, backflow time/gas production time, and backflow gas discharge time/gas production time curves under different interlayer pressure differences in the (**a**) commingled two-layer production and (**b**) commingled three-layer production.

Table 2. Summary of interference time and backflow volume in commingled multilayer production experiments.

Number of Commingled Production Layers	Commingled Layers	Ratio of Maximum to Minimum Layer Pressure	Total Gas Production Time (min)	Backflow Duration (min)	Ratio of Backflow Duration to Total Gas Discharge Time (%)	Interlayer Interference Time (min)	Ratio of Interlayer Interference Time to Total Gas Discharge Time (%)	Maximum Instantaneous Backflow Rate (mL/min)	Ratio of Maximum Instantaneous Backflow Rate to Gas Production Rate	Total Backflow Volume (mL)	Ratio of Total Backflow Volume to the Original Gas Volume in the Backflowed Layers (%)
2	Q5 + H8	3.01	1718	169	9.84	752	43.79	70.93	11.82	1511.00	61.17
	H8 + BX	1.14	1798	11	0.61	41	2.28	8.92	1.46	58.52	0.88
	S1 + TY	1.04	2068	3	0.14	6	0.29	1.53	0.24	8.55	0.12
3	Q5 + S2 + TY	3.21	2210	218 (Q5)	9.86	1306 (Q5)	59.10	110.01 (Q5)	14.67	2585.60 (Q5)	104.68
	Q5 + H8 + S2	3.12	2049	196 (Q5)	9.57	1160 (Q5)	56.61	109.61 (Q5)	14.24	2394.58 (Q5)	96.95
	H8 + S2 + TY	1.06	2500	8 (H8)	0.39	39 (H8)	1.56	4.92 (H8)	0.60	66.20 (H8)	0.99
	S2 + TY + BX	1.10	2200	12 (S2) + 2 (TY)	0.64	44 (S2) + 9 (TY)	2.41	12.93 (S2) + 1.41 (TY)	1.03	100.20 (S2) + 15.60 (TY)	1.50
4	Q5 + H8 + S1 + TY	3.21	2066	239 (Q5)	11.56	1351 (Q5)	65.39	176.09 (Q5)	15.58	2753.98 (Q5)	111.50
	H8 + S1 + S2 + TY	1.06	2683	12 (H8)	0.45	44 (H8)	1.64	8.30 (H8)	0.70	107.98 (H8)	1.62
	H8 + S2 + TY + BX	1.14	2164	17 (H8) + 5 (S2)	0.93	68 (H8) + 16 (S2)	3.56	12.03 (H8) + 2.77 (S2)	1.31	172.34 (H8) + 27.30 (S2)	2.92

The interference time also increases with a significant interlayer pressure difference as the number of commingled layers increases. The increase in the number of commingled layers leads to an increase in both gas backflow and the maximum instantaneous backflow rate, as well as an extended duration and volume of backflow, when the interlayer pressure ratio remains constant or similar. The larger the pressure ratio between layers, the more significant the observed increase.

3.3. Gas Recovery Efficiency and Interlayer Compatibility

In this work, the gas production coefficient together with its interference index is introduced to quantitatively assess the impact of commingled multilayer production on the gas production and recovery. The gas production coefficient W represents the incremental in gas recovery per unit pressure drop, while the interference index F measures the reduction ratio in W during commingled multilayer production compared to that of single-layer production. Their expressions are given as follows:

$$W = \Delta E_R / \Delta p_w \quad (1)$$

$$F = (W_1 - W_n)/W_1 \times 100\% \quad (2)$$

where ΔE_R is the incremental in gas recovery, %; Δp_w is the change in outlet pressure, MPa; and W_1 and W_n are the gas production coefficients for single-layer and multilayer extraction, respectively, MPa^{-1}.

3.3.1. Gas Production Coefficient

The results of single-layer depletion experiments for six layers are presented in Table 3. Figure 8a,b illustrates the relationship between the gas production coefficient and outlet pressure under single-layer depletion conditions for layer Q5 and layer H8. When the outlet pressure decreases, the gas production coefficient experiences an initial rapid increase, followed by a gradual decline during the stable production stage until reaching the terminal pressure. The gas production coefficient of layer H8 exhibits an initial upward trend, followed by a subsequent decline; however, the overall pattern is characterized by a more gradual change. During the single-layer depletion experiments, the gas recoveries of the layers Q5 and H8 are measured to be 81.80% and 93.26%, respectively, while the gas recovery in all other layers also exceeds 81.80%.

Table 3. Summary of gas production from single-layer depletion experiments.

Layer	Permeability ($\times 10^3$ μm^2)	Porosity (%)	Pressure (MPa)	Long Core Length (cm)	Gas Production Rate (mL)	Gas Recovery Efficiency (%)
Q5	0.76	8.17	7.30	47.40	2020.38	81.80
H8	0.66	7.80	22.00	42.40	6216.33	93.26
S1	0.45	6.05	22.60	42.40	6910.33	92.59
TY	0.56	8.70	23.40	43.40	4940.75	92.47
BX	0.85	7.08	25.00	22.00	3214.55	95.47
S2	0.54	6.90	22.80	42.40	7679.36	92.66

During commingled multilayer production, the gas production coefficients of either a high-pressure layer or a low-pressure layer have undergone significant changes. Such fluctuations in single-layer depletion and commingled two-layer production experiments of the Q5 + H8 layer are depicted in Figure 8a,b. During commingled production, the outlet pressure of the layer Q5 initially increases from its original formation pressure of 7.30 MPa to 12.48 MPa, characterized by a suppressed gas output due to interlayer interference until pressure equilibrium between the two layers is achieved and joint gas production is initiated. Compared to single-layer depletion, commingled production experiences a

more rapid decrease in the gas production coefficient, with an increase in pressure and a decrease in gas rate at a later stage. Although the layer H8 exhibits a higher gas discharge during commingled production, most of the gas is backflowed into the Q5 layer.

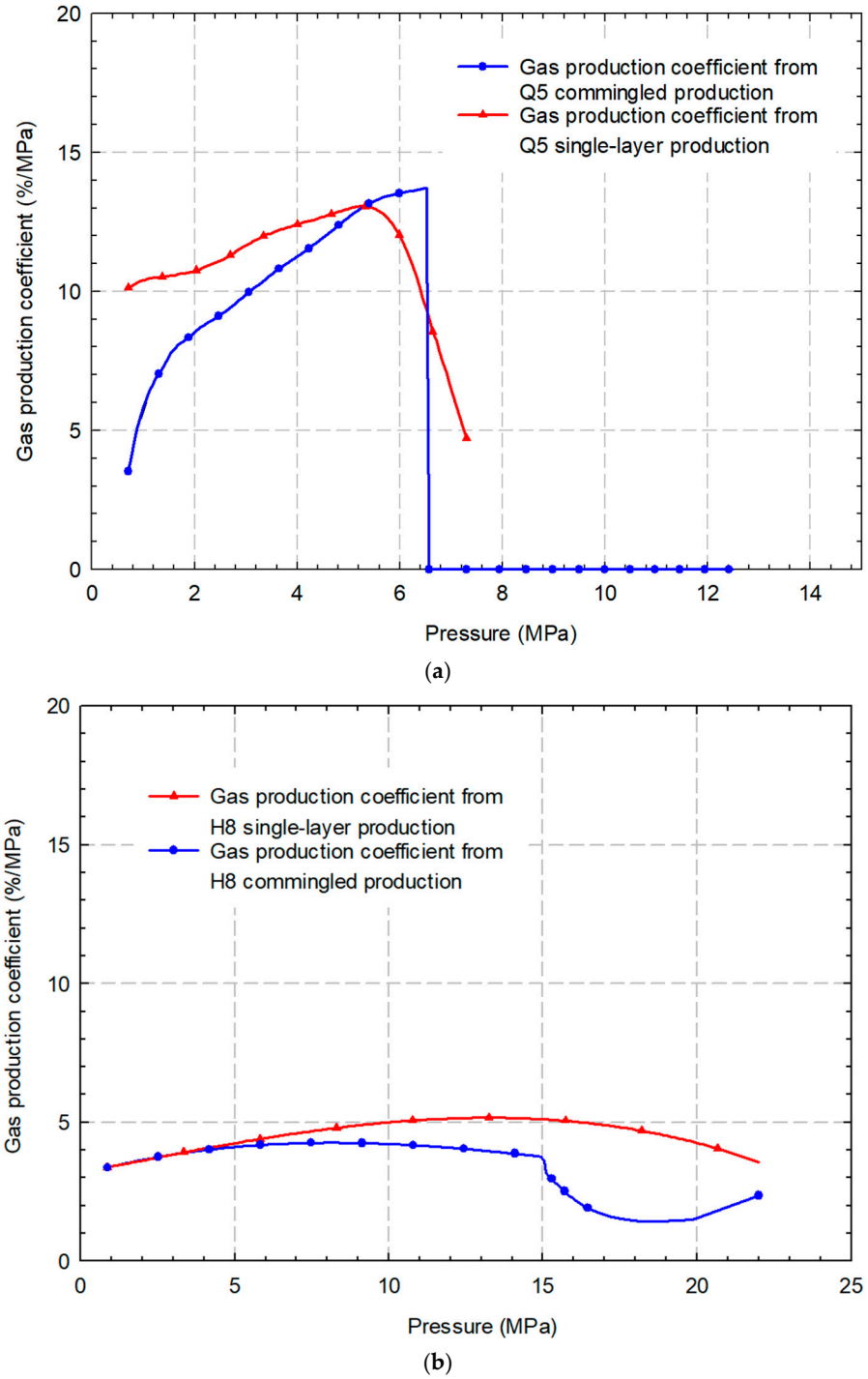

Figure 8. Gas production coefficients of (**a**) layer Q5 and (**b**) layer H8 in commingled two-layer (Q5 + H8 layer) production experiments, together with their corresponding single-layer depletion experiments.

3.3.2. Interference Index and Commingled Production Loss Ratio

The interference index and gas production loss ratio for each layer during commingled multilayer production are tabulated in Table 4. The gas production loss ratio during commingled production refers to the ratio of the total gas production to the cumulative

production from the single-layer depletion experiments of the corresponding layers. In the case of commingled two-layer production of the Q5 + H8 layer, its interference indices for the layers Q5 and H8 are, respectively, calculated to be 28.28 and 6.57, resulting in an overall gas production loss ratio of 10.95%. During the commingled H8 + BX layer production, the interference index is relatively lower, resulting in a 6.67% reduction in gas output compared to that of single-layer production. Compared to single-layer production, the commingled production of the BX + TY layers exhibits a comparatively smaller variation in gas output with an insignificantly low rate of gas production loss.

Table 4. Summary of interference index and gas production loss ratio.

Number of Commingled Production Layers	Commingled Layers	Initial Gas Production Rate (mL/min)	Interference Index (%)	Commingled Production Loss Ratio (%)
2	Q5	5.3	28.28	10.95
	H8		6.57	
	H8	6.1	9.07	6.67
	BX		2.06	
	S1	6.5	−0.6	0.08
	TY		1.10	
3	Q5	7.7	36.54	12.27
	H8		8.53	
	S2		8.93	
	Q5	7.5	38.24	13.1
	S2		8.98	
	TY		9.24	
	H8	8.2	0.06	0.26
	S2		0.03	
	TY		0.87	
	S2	8.3	12.51	8.16
	TY		4.88	
	BX		2.80	
4	Q5	11.8	44.33	13.36
	H8		9.10	
	S1		10.09	
	TY		10.61	
	H8	11.9	0.53	0.52
	S1		0.36	
	S2		0.08	
	TY		0.95	
	H8	11.3	15.58	8.98
	S2		9.78	
	TY		1.96	
	BX		5.11	

In the case of commingled three-layer production for the Q5 + H8 + S2 and Q5 + S2 + TY layers, the interference index is relatively high, with the layer Q5 being the most

significantly affected one. The respective gas production loss ratios are calculated to be 12.27% and 13.10%. For the commingled production for the S2 + TY + BX layers, the interference index in the affected S2 layer reaches 12.51%, resulting in a gas production loss ratio of 8.16%. The interference index is relatively low for the commingled production from the H8 + S2 + TY layers.

For the case of commingled four-layer production for the Q5 + H8 + S1 + TY layers, the gas recovery of layer Q5 is decreased from 81.80% in single-layer depletion production to 45.54%, with the interference index up to 44.33%, indicating a high level of interference, and its overall gas production loss ratio is 13.36%. In contrast, the commingled production from the H8 + S2 + TY + BX layers exhibits two interfered layers, with the primary affected layer H8 having an interference index of 15.58% and the secondary affected layer S2 having an interference index of 9.78%, with an overall gas production loss ratio of 8.98%. The interference level in commingled production for the H8 + S1 + S2 + TY layers is relatively low, resulting in minimal loss of gas production.

The observation reveals that, during a commingled multilayer production, an increase in interlayer differences leads to a higher interference index, resulting in a greater loss ratio of commingled production gas rates and a reduced proportion of gas production from the low-pressure layer. When the pressure difference of the commingled layers is similar, an increase in the number of commingled layers will result in an escalation of interference time, backflow gas volume, and backflow rate. Consequently, this amplifies the degree of interference, ultimately leading to a decline in overall gas production and an elevation in commingled production gas loss ratio [23–25].

3.3.3. Commingled Production Compatibility

The aforementioned analysis clearly indicates that the interlayer pressure difference plays a pivotal role in determining the extent of interlayer interference and its impact on gas production and recovery. Therefore, it serves as a fundamental indicator for evaluating the compatibility of commingled multilayer production.

Of the existing six interlayers, the middle four ones (i.e., layers H8, S1, S2, and TY) are found to be suitable for commingled production. The gas contribution ratios of each layer for commingled three-layer production of the three scenarios are illustrated in Figure 9a–c. It can be observed that the H8, S1, S2, and TY layers demonstrate minimal interlayer differences, small interference indices, and comparable production contribution ratios during commingled production. Consequently, this leads to a prolonged stable production duration and favorable compatibility in commingled production.

The Q5 and BX layers are not suitable for commingled production with the other layers. Due to the lower pressure of the layer Q5, a significant interlayer interference arises during commingled production, resulting in an extended period of interference and a shortened phase of stable production, ultimately leading to a reduction in overall gas production. The high permeability and initial pressure of the BX layer result in interference with the other layers. Due to the limited initial reserves of the BX layer, however, there is a rapid decline in both the gas production rate and production contribution ratio, leading to a shortened gas production period and stable production stage. Consequently, this ultimately results in an overall reduction in gas production compared to single-layer extraction.

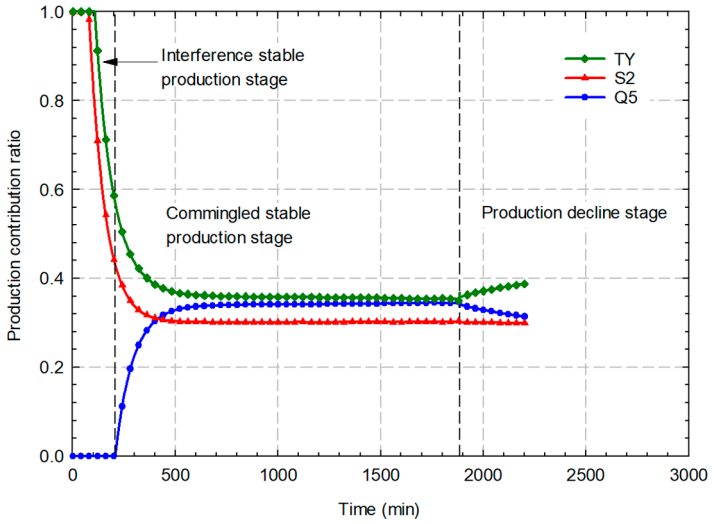

(**a**)

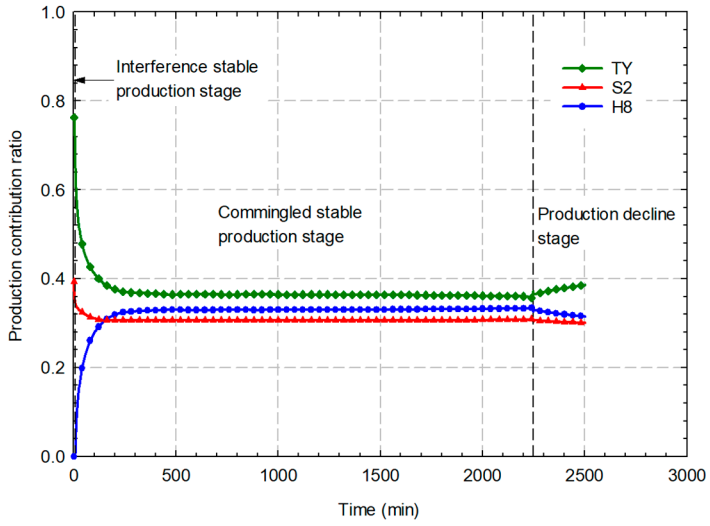

(**b**)

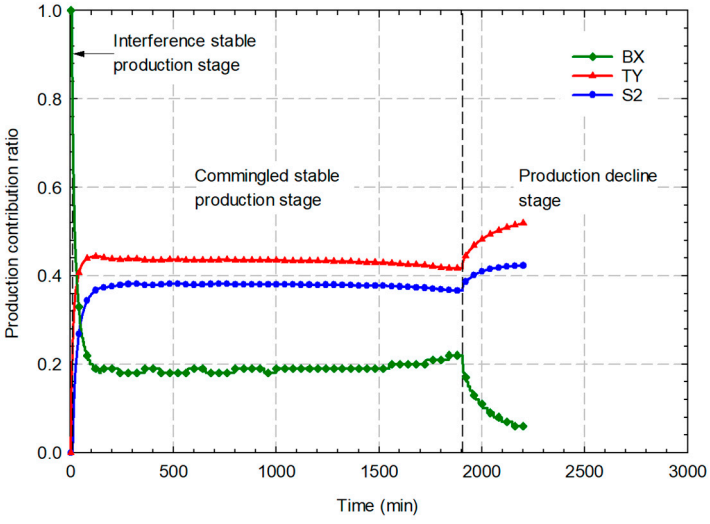

(**c**)

Figure 9. Production contribution ratio curves for the commingled production: (**a**) Q5 + S2 + TY layers; (**b**) H8 + S2 + TY layers; and (**c**) S2 + TY + BX layers.

4. Conclusions

(1) The gas production characteristics of commingled multilayer production can be categorized into three stages, i.e., the production stage with stable interference from each interlayer, stable production from commingled layers, and the production decline stage from commingled layers. During the production stage with stable interference from each interlayer, there is a gas backflow occurring from a high-pressure layer to a low-pressure layer. Subsequently, in the stable production stage with commingled layers, all layers produce gas continuously. During the production decline stage, there is a gradual reduction observed in the commingled production rate.

(2) The greater the difference in interlayer pressure, the more pronounced the disparities in backflow time, the ratio of backflow time to gas production time, and the ratio of backflow gas discharge time to gas production time. The experiments demonstrated a range of backflow time to gas production time ratios, spanning from 0.14% to 9.84%. The ratio between the duration of backflow gas discharge and the duration of gas production in the experiments spans from 0.29% to 53.22%, and the volumetric ratio of backflow volume to the original gas volume is varied from 0.12% to 86.15%.

(3) Under conditions where the pressure differentials between commingled layers are similar, as the number of commingled layers increases from two to four, there is an escalation in the interference index for the gas production coefficient and a corresponding rise in the gas loss ratio from 10.95% to 13.36%, intensifying the interlayer interference and ultimately resulting in an overall reduction in gas production, with a more pronounced decrease observed in low-pressure layers. Therefore, it is imperative to minimize the number of interfered layers during commingled multilayer production.

(4) The H8, S1, S2, and TY layers exhibit a minimal interlayer pressure difference, negligible interference index, and suitable compatibility for commingled production. Since the initial pressure of the layer Q5 is lower and the layer BX is characterized by its high permeability, high original pressure, and limited original reserves, both layers are unsuitable for commingled production with other layers.

Author Contributions: Conceptualization, Y.L., J.W., J.L. and D.Y.; methodology, Y.L., W.H., J.L., H.S. and D.Y.; validation, W.H., J.W. and J.L.; formal analysis, Y.L., W.H., J.W., J.L., H.S. and D.Y.; investigation, Y.L., J.W. and D.Y.; resources, Y.L., J.W., J.L. and D.Y.; data curation, Y.L., W.H., J.W., J.L. and H.S.; writing—original draft preparation, Y.L. and W.H.; writing—review and editing, Y.L., W.H., J.W., J.L., H.S. and D.Y.; funding acquisition, Y.L. and D.Y. All authors have read and agreed to the published version of the manuscript.

Funding: National Natural Science Foundation of China (Grant No.: 52274049) and Natural Sciences and Engineering Research Council of Canada (NSERC) (Discovery Grant and Collaborative Research and Development (CRD) Grant).

Data Availability Statement: The original contributions presented in the study are included in the article, further inquiries can be directed to the corresponding author.

Conflicts of Interest: Authors Jingjian Wang and Jiaojiao Liu were employed by Changqing Oilfield Company. The remaining authors declare that the research was conducted in the absence of any commercial or financial relationships that could be construed as a potential conflict of interest.

References

1. Cheng, M.; Xue, W.; Guo, Z.; Hou, M.; Wang, C. Development of large-scale tight gas sandstone reservoirs and recommendations for stable production—The example of the Sulige gas field in the Ordos Basin. *Sustainability* **2023**, *15*, 9933. [CrossRef]
2. Wu, X.; Liu, Q.; Zhu, J.; Li, K.; Liu, G.; Chen, Y.; Ni, C. Geochemical characteristics of tight gas and gas-source correlation in the Daniudi gas field, the Ordos Basin, China. *Mar. Pet. Geol.* **2017**, *79*, 412–425. [CrossRef]
3. Wu, H.; Ji, Y.; Liu, R.; Zhang, C.; Chen, S. Insight into the pore structure of tight gas sandstones: A case study in the Ordos Basin, NW China. *Energy Fuels* **2017**, *31*, 13159–13178. [CrossRef]
4. Jia, S.; Yang, J.; Sun, T.; Edrisi, A.R.; Chen, Y.; Chen, K.; Wen, Z. Multilayer commingled production effects in hydrate reservoirs with underlying gas. *Processes* **2024**, *12*, 1225. [CrossRef]

5. Yang, H.; Yue, P.; Wang, Z.; Wang, M.; Chen, Y.; Zhou, Y.; Qu, S. Experimental evaluation of the succession sequence during commingled production in a tight gas reservoir. In Proceedings of the International Field Exploration and Development Conference, Wuhan, China, 20–22 September 2024; pp. 122–138.
6. Hou, B.; Cui, Z.; Ding, J.; Zhang, F.; Zhuang, L.; Elsworth, D. Perforation optimization of layer-penetration fracturing for commingling gas production in coal measure strata. *Pet. Sci.* **2022**, *19*, 1718–1734. [CrossRef]
7. Santiago, V.; Ribeiro, A.; Hurter, S. Modeling the contribution of individual coal seams on commingled gas production. *SPE Prod. Oper.* **2021**, *36*, 245–261. [CrossRef]
8. Sui, Y.; Cui, C.; Wang, Z.; Yang, Y.; Jia, P.; Wang, X. Production splitting method for commingled production reservoir based on automatic history matching of single well. *Lithosphere* **2022**, *2022*, 9225890. [CrossRef]
9. Nie, S.; Li, J.; Liu, K.; Zhong, X.; Wang, Y. Numerical evaluation of commingled production potential of marine multilayered gas hydrate reservoirs using fractured horizontal wells and thermal fluid injection. *J. Mar. Sci. Eng.* **2024**, *12*, 365. [CrossRef]
10. Hou, J.; Zhao, L.; Zhao, W.; Feng, Z.; Wang, X.; Zeng, X. Evaluation of pore-throat structures of carbonate reservoirs based on petrophysical facies division. *Front Earth Sci.* **2023**, *11*, 1164751. [CrossRef]
11. Zhang, T.; Wang, B.; Zhao, Y.; Zhang, L.; Qiao, X.; Zhang, L.; Guo, J.; Thanh, H.V. Inter-layer interference for multi-layered tight gas reservoir in the absence and presence of movable water. *Pet. Sci.* **2024**, *21*, 1751–1764. [CrossRef]
12. Wang, L.; He, Y.; Wang, Q.; Liu, M.; Jin, X. Improving tight gas recovery from multi-pressure system during commingled production: An experimental investigation. *Nat. Resour. Res.* **2021**, *30*, 3673–3694. [CrossRef]
13. Chai, X.; Tian, L.; Dong, P.; Wang, C.; Peng, L.; Wang, H. Study on recovery factor and interlayer interference mechanism of multilayer co-production in tight gas reservoir with high heterogeneity and multi-pressure systems. *J. Pet. Sci. Eng.* **2022**, *210*, 109699. [CrossRef]
14. Tao, X.; Okere, C.J.; Su, G.; Zheng, L. Experimental and theoretical evaluation of interlayer interference in multi-layer commingled gas production of tight gas reservoirs. *J. Pet. Sci. Eng.* **2022**, *208*, 109731. [CrossRef]
15. Zhao, X.; Luo, D.; Zheng, Y.; Xia, L. Ordering the exploitation of heterogeneous carbonate gas reservoirs. *J. Porous Media* **2019**, *22*, 1595–1607. [CrossRef]
16. Hu, Y.; Li, X.; Jiang, L.; Wan, Y.; Guo, C.; Jiao, C.; Chai, X.; Jing, W.; Xu, X.; Zhou, M.; et al. Production experiment of multi-layer edge-water loose sandstone gas reservoir in Qaidam Basin. *Nat. Gas Geosci.* **2022**, *33*, 1499–1508.
17. Liu, G.; Meng, Z.; Luo, D.; Wang, J.; Gu, D.; Yang, D. Experimental evaluation of interlayer interference during commingled production in a tight sandstone gas reservoir with multi-pressure systems. *Fuel* **2020**, *262*, 116557. [CrossRef]
18. Guo, C.; Qin, Y.; Sun, X.Y.; Wang, S.Q.; Xia, Y.C.; Ma, D.M.; Bian, H.; Shi, Q.; Chen, Y.; Bao, Y.; et al. Physical simulation and compatibility evaluation of multi-seam CBM co-production: Implications for the development of stacked CBM systems. *J. Pet. Sci. Eng.* **2021**, *204*, 108702. [CrossRef]
19. Tang, H.; Zhang, K.; Tang, R.; Lu, D.; Tan, L. The essence and re-recognition of interlayer interference. *J. Southwest Pet. Univ. (Sci. Technol. Ed.)* **2022**, *44*, 113–124.
20. Jiang, B.; Cheng, S.; Kang, B.; Gao, Y.; Ma, K. Productivity evaluation method of multi-layer sandstone reservoir based on dynamic prediction of interlayer interference. *Pet. Geol. Recovery Effic.* **2022**, *29*, 124–130.
21. He, M. Study on Quantitative Interpretation of Production Profile of Multi-Layer Commingled Production of Coalbed Methane Wells in Fukang Mining. Master's Thesis, China University of Petroleum (Beijing), Beijing, China, 2021.
22. Ji, H. Research on Sedimentary Facies and Sand Body Distribution of Neopaleozoic Reservoir in Sulige Area of the Ordos Basin. Master's Thesis, China University of Geosciences (Beijing), Beijing, China, 2007.
23. Wang, C. Research on Interlayer Interference Mechanism in Offshore Light Oil Reservoir. Master's Thesis, China University of Petroleum (Beijing), Beijing, China, 2020.
24. Fu, Y.; Chen, J.; Zhang, R.; Shi, L.; Tang, J.; Wang, X.; Cao, X.; Qian, H.; Liu, R.; Li, Z. Characterization of interlayer interference coefficient before layered oil recovery. *Energy Conserv. Pet. Petrochem. Ind.* **2022**, *12*, 1–4.
25. Zhang, C.; Guo, H.; Chen, X. Analysis of interlayer interference phenomenon of commingled reservoir development process with depletion development. *Petrochem. Ind. Appl.* **2015**, *34*, 35–39.